IEEE Access
Multidisciplinary | Rapid Review | Open Access Journal

Received 18 December 2022, accepted 24 December 2022, date of publication 28 December 2022,
date of current version 11 January 2023.

Digital Object Identifier 10.1109/ACCESS.2022.3232819

RESEARCH ARTICLE

Research on the Influence of Model Surface Conductivity on RCS Test Accuracy

WU YACONG, HUANG JUN, AND SONG LEI
School of Aeronautic Science and Engineering, Beihang University, Beijing 100083, China
Corresponding author: Song Lei (songlei@buaa.edu.cn)

ABSTRACT The accuracy of the RCS (Radar Cross Section) test is closely related to the conductivity of the model surface. The Chinese military standard has stringent surface resistance criteria for models. If the resistance criteria are appropriately relaxed, model processing can be more effective and expenses can be reduced. However, there are few quantitative evaluations of the relationship between surface resistance and RCS test error, making it impossible to design the model surface resistance in accordance with RCS test accuracy requirements. In this paper, firstly, the influence of model surface resistance on RCS is clarified through theoretical, simulation, and experimental research. The RCS analysis approach of the finite conductivity model is established. Subsequently, taking various typical shapes as research objects, such as the sphere, cube, flying wing aircraft, wing-body combination, and stealth aircraft, the simulation analysis of radar scattering characteristics is carried out under varied sheet resistances and multiple frequencies. A more attainable surface conductivity control standard for the RCS test model has been formulated, which is relaxed by 93% and 727% for models with average RCS of less than and higher than -30dBsm compared with the indicator in the Chinese military standard.

INDEX TERMS Surface resistance, RCS test model, quantitative analysis, Chinese military standard, accuracy requirement.

I. INTRODUCTION

Model processing is an essential part of RCS testing. Compared with traditional sheet metal processing, emerging processing techniques such as 3D printing can better fulfill current experimental needs due to their high precision, high efficiency, and low cost [1], [2].

According to the current Chinese military standard (GJB5022-2001) [3], the resistance measured between two points on the surface of the RCS test model at intervals of 300 mm should be less than 1 ohm. For weight, price-performance ratio, and molding process considerations, 3D printing models for RCS tests are typically made of insulating materials with a layer of conductive paint sprayed on the surface to provide conductivity [4], [5]. However, the time and cost required to use this method to meet the requirements of GJB5022-2001 are relatively high.

The associate editor coordinating the review of this manuscript and approving it for publication was Chan Hwang See.

However, most of the current research [6] on the influence of model surface resistance on RCS is focused on qualitative analysis. If the quantitative relationship between surface resistance and RCS testing error can be established, the conductivity of the model surface can be determined according to the test accuracy requirements, thereby reducing the processing difficulty.

In order to solve the problems mentioned above and make emerging processing technology more accessible to RCS test models, this paper aims to explain the influence of model surface resistance on RCS quantitatively; and establish an RCS analysis method for complex finite conductivity models through theoretical, simulation and experimental research. According to the simulation analysis of radar scattering characteristics at different frequencies for a variety of typical shapes, a more accessible implemented surface resistance standard of the RCS test model is developed based on the actual test conditions of the general compact range in the anechoic room [7].

II. RESEARCH ON THE INFLUENCE OF SHEET RESISTANCE ON RCS

For the general 3D processing RCS test model, the conductivity is entirely provided by the conductive paint on the surface. Due to wave-transmissive [8], the internal insulating structure has no effect on the RCS test. The conductive paint on the outer layer can be regarded as a conductive film since the thickness is small enough relative to the size. Consequently, the conductive film is directly used as the research object in section 2.

A. THEORETICAL EXPLANATION OF THE CORRELATION BETWEEN SURFACE RESISTANCE AND RCS

RCS can be defined by the scattered field at the radar receiving antenna and the incident field at the target as [9]

$$\sigma = \lim_{R\to\infty} 4\pi R^2 \frac{|E_S|^2}{|E_I|^2} = \lim_{R\to\infty} 4\pi R^2 \frac{|H_S|^2}{|H_I|^2} \tag{1}$$

where R is the distance between the target and radar receiving antenna, E_S, H_S are the electric and magnetic field strength of the scattered echo at the radar receiving antenna, and E_I, H_I are the electric and magnetic field strength of the incident wave.

Meanwhile, the reflection coefficient represents the ratio of the reflected electric or magnetic field to the incident electric or magnetic field. As a result, the influence of the film's conductivity on RCS that we are concerned about is the influence of the film's conductivity on the reflection coefficient.

According to the literature [10], [11], the reflection coefficient of a conductive film with the thickness of d and the conductivity of σ can be expressed as:

$$R = \frac{\alpha - \beta}{(\alpha + 1)(\beta + 1)} \tag{2}$$

where $\alpha = \frac{i\omega\mu_0 d}{2\eta_0}$, $\beta = \frac{\sigma\eta_0 d}{2}$, $\omega = 2\pi f$ represents the angular frequency, $\mu_0 = 8.85 \times 10^{-12}$ is the permeability of vacuum and $\eta_0 \approx 377\Omega$ is the impedance of free space, σ stands for conductivity.

Assuming a conductive film with thickness of 20 μm and conductivity of $10^3 S/m$, the magnitude of α and β under different bands are shown in TABLE 1.

TABLE 1. Magnitude of α and β under different bands.

Band	Frequency	magnitude of α	magnitude of β
P-band	300MHz	10^{-10}	1
L-band	1GHz	10^{-9}	1
S-band	3GHz	10^{-9}	1
C-band	6GHz	10^{-9}	1
X-band	10GHz	10^{-8}	1
Ka-band	30GHz	10^{-7}	1

As can be seen in the TABLE 1, the value of α can be ignored compared with β since in the range of P-band to Ka-band, the magnitude of α and β differs by 10^{-7} at least. Thus, simplify the Eq.(2) to get the reflectivity of the conductive film:

$$R = (1 + \frac{2}{\sigma\eta_0 d})^{-1} = (1 + \frac{2Rs}{\eta_0})^{-1} \tag{3}$$

where $Rs = \frac{\rho}{d} = \frac{1}{\sigma d}$ represents the sheet resistance of the conductive film, which is a physical quantity used to characterize the resistivity of film and the unit is $\Omega/\square$, ρ stands for resistivity.

According to Eq.(3), the reflection coefficient is only directly related to the sheet resistance of the conductive film, as with the radar scattering characteristics.

B. SIMULATION ANALYSIS AND EXPERIMENTAL VERIFICATION OF THE INFLUENCE OF SHEET RESISTANCE ON RCS

To further discuss the influence of resistance on RCS under different incident angles, in this part, the ITO (Indium Tin Oxide) conductive film with different square resistances is taken as the research object, and this problem is further analyzed and verified through computational electromagnetic simulation and compact field test methods. The ITO conductive film is produced by the magnetron sputtering process [12], and the sheet resistance is controllable and uniform, making it ideal for quantitative analysis and repeated tests [13], [14].

The arithmetic average of RCS is commonly employed to express the radar scattering characteristics of a target within a specific angle range since RCS fluctuates with the incidence angle. The average value of the RCS in the forward, lateral, and backward directions is defined as the mean value of the RCS within ±30 degrees around the 0-degree incident angle, 90-degree incident angle, and 180-degree incident angle [15].

Simulations are performed using ITO conductive films measuring 0.3 meters in length and 0.2 meters in breadth. Four different sheet resistances are selected for the simulation. The film's number and sheet resistance are shown in Table 2. As illustrated in Fig.1, the incident wave is

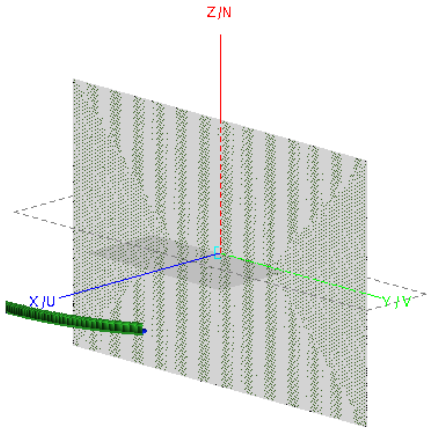

FIGURE 1. Simulation model of ITO conductive film.

vertically polarized, with an incident angle ranging from −30 to 30 degrees. As a reference, an aluminum plate of the same size is also selected for simulation to determine the difference between the RCS of ITO conductive films with varied sheet resistances and the RCS of the metal model.

Meanwhile, experiments using ITO conductive films are carried out to evaluate the accuracy of the simulation method, with the same experimental settings as the simulation. For the convenience of testing, the ITO conductive film is attached to the insulating glass plate by the magnetron sputtering process to simulate conductive paint sprayed on the insulating model [16], as illustrated in Fig.2.

The RCS test [17] is conducted in an anechoic room that simulates free-space and far-field conditions. The compact range has a quiet zone with a size of $\Phi 2.5m \times 2.5m$, a background level lower than −80dBsm, and a test error of less than 0.5dB for targets greater than −50dBsm.

TABLE 2. Comparison between simulation and measured RCS.

Number	Sheet resistance ($\Omega/\square$)	Forward RCS average		
		Simulation value (dBsm)	Test value (dBsm)	Error (dB)
Metal	0	3.7949	3.7454	0.0494
ITO #1	1.5	3.7226	3.5919	0.1306
ITO #2	6.1	3.5054	3.4238	0.0816
ITO #3	13.5	3.1691	3.1731	-0.0041
ITO #4	50	1.6980	1.6918	0.0063

The comparison between the simulation and measured value of forward RCS average for #1∼#4 ITO conductive films and aluminum plate are shown in Table 2 and Fig.3∼Fig.7. The figure's title is composed of two parts: "ITO#1" denotes the ITO conductive film number, and "Rs1.5" denotes the sheet resistance.

The difference between the forward RCS average of the ITO conductive film and the aluminum plate reduces as the sheet resistance decreases. The difference is only about 0.07dB when the sheet resistance is $1.5\Omega/\square$. The simulation value is nearly identical to the test value, with an error of less than 0.15dB, demonstrating the accuracy of the RCS simulation method for the finite conductivity model and the theoretical framework established in this paper for the influence of the sheet resistance of the model surface on the radar scattering characteristics.

FIGURE 2. RCS test of ITO conductive film.

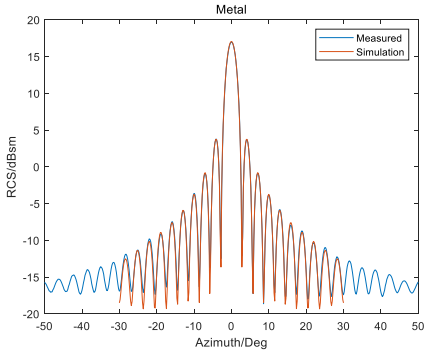

FIGURE 3. Comparison between simulation and test for metal plate.

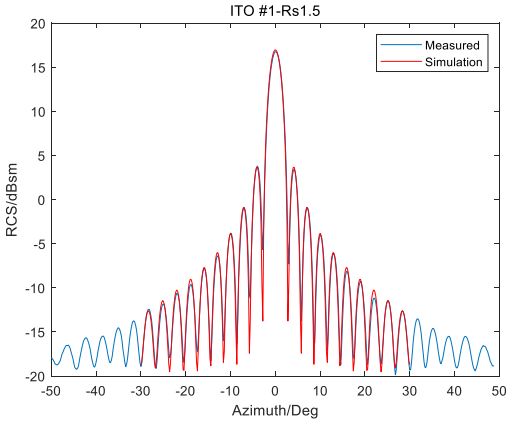

FIGURE 4. Comparison between simulation and test for ITO #1.

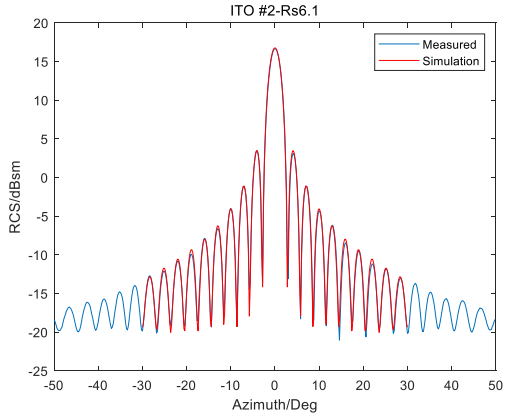

FIGURE 5. Comparison between simulation and test for ITO #2.

C. QUANTITATIVE ANALYSIS OF THE INFLUENCE OF SHEET RESISTANCE ON RCS

To further quantify the influence of sheet resistance on RCS, the ITO conductive film, which can be regarded as a simple plate model, is utilized for quantitative simulation

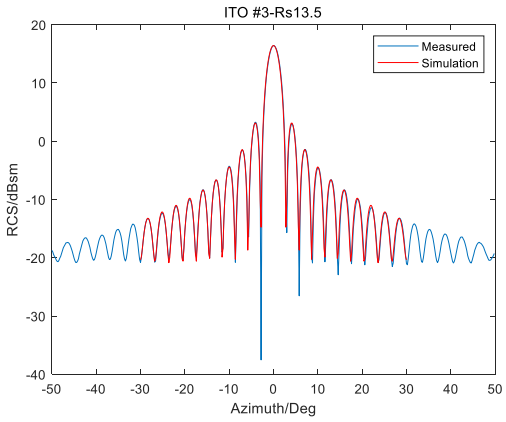

FIGURE 6. Comparison between simulation and test for ITO #3.

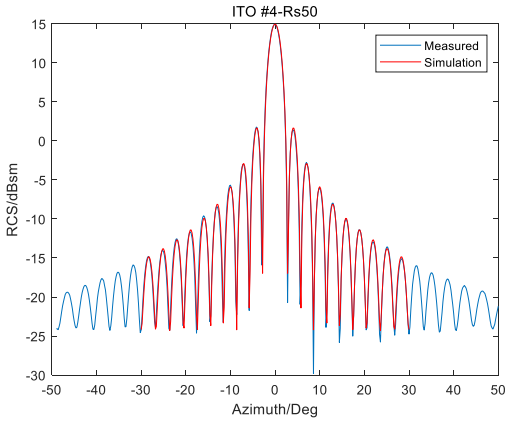

FIGURE 7. Comparison between simulation and test for ITO #4.

analysis after establishing the RCS analysis method of the finite conductivity model and validating it with the RCS test.

It should be noted that the indicator in the Chinese military standard is the resistance between two points on the model surface, and its relationship with the sheet resistance has been proven in another paper by the author. Since sheet resistance can be employed directly in RCS simulation, the sheet resistance is used to characterize the conductivity of the model surface in this paper. The indicator specified in the Chinese military standard is also stated as 0.725 Ω/□ in sheet resistance. The author describes the specific theoretical derivation procedure in another paper. [18].

To establish a more intuitive mapping relationship between sheet resistance and RCS, the average forward RCS value of ITO conductive film is calculated for a range of sheet resistances from 0 to 50 Ω/□ and compared with that of a PEC (Perfect Electric Conductor) plate. As depicted in Fig.8, the difference between the forward RCS average of the ITO conductive films with varied sheet resistances and the PEC plate can be acquired to construct the curve of the difference against sheet resistance. When the difference is smaller than the permissible test error, the test model under the current sheet resistance can be considered to meet the conductivity requirements.

In Fig.8, the right figure is an enlargement of the red box on the left figure, and the star indicates the difference corresponding to the sheet resistance value specified in GJB5022-2001. As described in the figure, the difference is significantly reduced with the decrease of the sheet resistance until it reaches the star mark. After that, the difference tends to change gradually.

The forward RCS average of the model with sheet resistance specified by the GJB5022-2001 is quite close to that of the PEC model, with a difference of only 0.035dB for the plate model. If the actual test accuracy is limited, the model's surface resistance criteria can be appropriately relaxed.

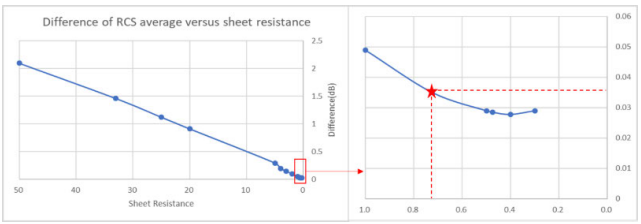

FIGURE 8. Difference of RCS average versus sheet resistance for plate model.

III. SIMULATION ANALYSIS OF THE ACCEPTABLE SHEET RESISTANCE FOR VARIOUS SHAPES AND MULTIPLE FREQUENCIES

As previously stated, the model's sheet resistance impacts the reflection and transmission coefficients. For the plate model, the transmitted electromagnetic wave enters the free space without encountering other conductive surfaces; for the complex model, the transmitted electromagnetic wave will be reflected and transmitted numerous times in the cavity within the model [19], [20]. The impact of sheet resistance on RCS must also consider factors such as the model's complex shape and the incident wave's frequency.

In section 2, simulation analysis and experimental verification are carried out with the plate model as the research object. The electromagnetic simulation method for the finite conductivity model is established, and the influence of the surface resistance on the model RCS is clarified. In section 3, the simulation method of the finite conductivity model is used to conduct RCS analysis of various shapes at multiple frequencies. The curves of average RCS versus sheet resistance are plotted separately to obtain the acceptable sheet resistance range for each model.

The specific simulation method for each model is as follows:

1. Establish the simulation model of corresponding sheet resistance within the range of 0-10Ω/□ with an interval of 0.1Ω/□, and calculate the forward, lateral and backward RCS average of the model under the sheet resistance;

2. Establish the simulation model of PEC, and calculate the forward, lateral and backward RCS average of the PEC model;

3. Plot the curve of forward, lateral and backward RCS average values versus sheet resistance. The blue curve represents the RCS of the model with different sheet resistances, and the red dotted line represents the RCS of the PEC model. The closer the two curves are, the smaller the test error under the current sheet resistance.

4. Establish the upper and lower error limits within ±1dB based on the RCS of the PEC model. The error under the specific sheet resistance is considered acceptable when the RCS value is within limits.

A. INFLUENCE OF SHAPE ON SURFACE CONDUCTIVITY REQUIREMENTS

In this part, simulations are performed for typical shapes such as the sphere, cube, flying wing aircraft, wing-body combination, and stealth aircraft to develop a surface resistance control standard suitable for most shapes.

The curves of average RCS versus sheet resistance are derived using the simulation method described above; the maximum acceptable sheet resistance of each shape is summarized in Table 3. The lower the RCS of the model itself, the higher the requirements for surface conductivity. By analyzing the acceptable sheet resistance of five typical shapes, the conclusion can be drawn as follows: The highest required sheet resistance is 1.4Ω/□, with the corresponding average RCS of −52.55dBsm and −36.91dBsm, respectively.

TABLE 3. Maximum acceptable sheet resistance of typical shapes.

	Average RCS	Maximum sheet resistance	Average RCS	Maximum sheet resistance
	Sphere		Cube	
Forward	-15.22	All	2.03	All
Lateral	\	\	\	\
Backward	\	\	\	\
	Flying wing aircraft		Wing-body combination	
Forward	-52.55	1.4	-36.91	1.4
Lateral	-38.44	All	-8.36	All
Backward	-49.02	4.7	-9.76	All
	Stealth aircraft			
Forward	-22.28	All	Note: "All" means that the sheet resistance within the calculation range is acceptable	
Lateral	-22.88	All		
Backward	-34.36	8.9		

1) VARIATION OF AVERAGE RCS OF SPHERE MODEL WITH SHEET RESISTANCE

The sphere model with a diameter of 0.2 meters is shown in Fig.9. Only the forward RCS average is compared due to symmetry. According to Fig.10, within the calculated sheet resistance range (0∼10Ω/□), the difference of average RCS between the calculated model and the PEC model is controlled within 1dB.

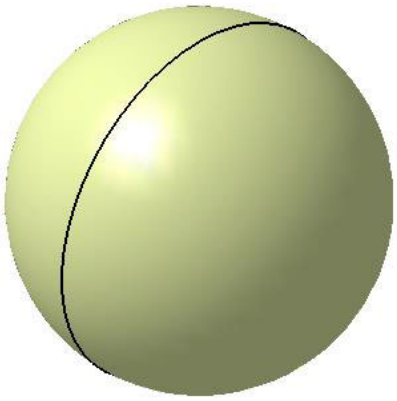

FIGURE 9. Sphere model.

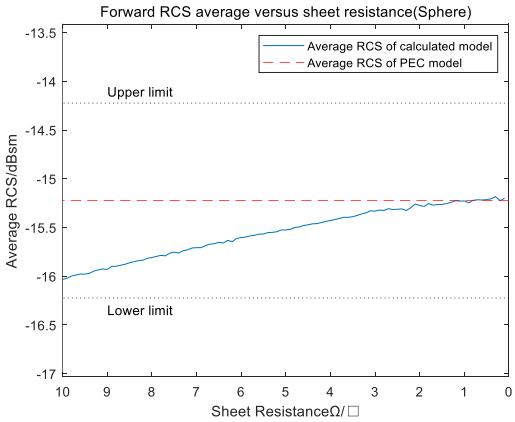

FIGURE 10. Forward RCS average versus sheet resistance (Sphere).

2) VARIATION OF AVERAGE RCS OF CUBE MODEL WITH SHEET RESISTANCE

The cube model with a side length of 0.2 meters is shown in Fig.11. In view of symmetry, only the forward RCS average is compared. According to Fig.12, within the calculated sheet

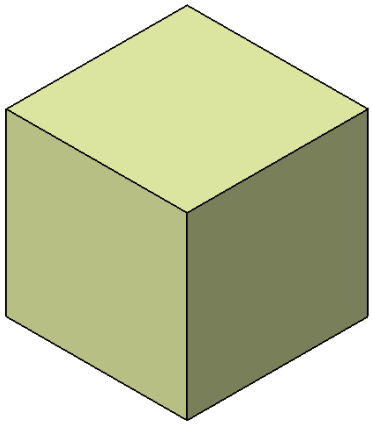

FIGURE 11. Cube model.

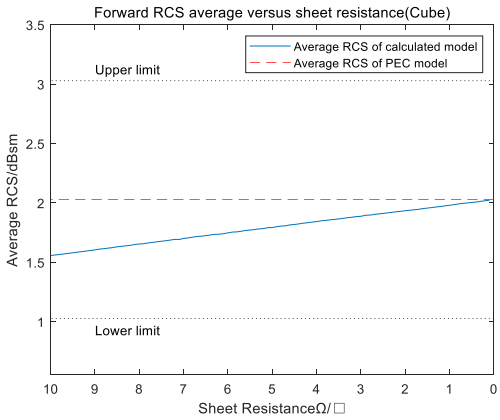

FIGURE 12. Forward RCS average versus sheet resistance (Cube).

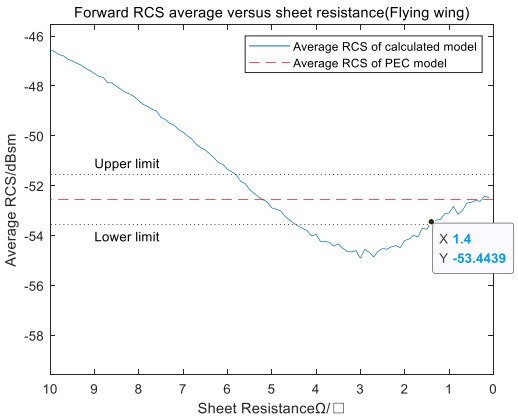

FIGURE 14. Forward RCS average versus sheet resistance (Flying wing).

resistance range (0∼10Ω/□), the discrepancy in average RCS between the calculated model and the PEC model is controlled within 1dB.

3) VARIATION OF AVERAGE RCS OF FLYING WING AIRCRAFT WITH SHEET RESISTANCE

The flying wing aircraft model with a length of 0.22 meters and a wingspan of 0.209 meters is shown in Fig.13. The forward, lateral, and backward RCS of the model are compared to those of the PEC model. Since the forward RCS of the flying wing aircraft is as low as -52.55dB, the relative error under the same absolute error is substantially larger, necessitating the absolute error in the RCS test to be as small as feasible, namely, the conductivity of model surface needs to be closer to the PEC model. The maximum acceptable sheet resistance is selected to be 1.4Ω/□ based on the forward, lateral, and backward RCS limitations (Fig.14∼ Fig.16).

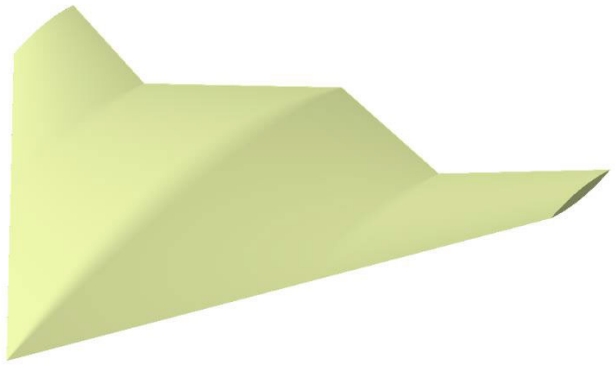

FIGURE 13. Flying wing aircraft model.

5. Evaluate the forward, lateral, and backward RCS error thoroughly, and summarize the acceptable sheet resistance value range.

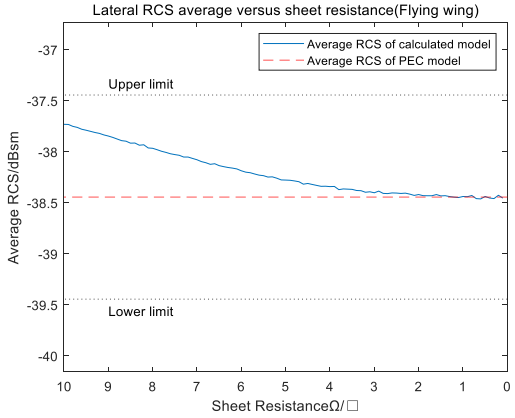

FIGURE 15. Lateral RCS average versus sheet resistance (Flying wing).

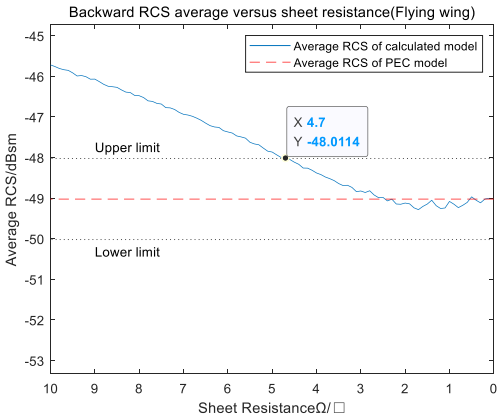

FIGURE 16. Backward RCS average versus sheet resistance (Flying wing).

4) VARIATION OF AVERAGE RCS OF WING-BODY COMBINATION WITH SHEET RESISTANCE

The wing-body combination model with a length of 1.192 meters and a wingspan of 0.889 meters is shown in Fig.17. Considering the forward, lateral, and backward RCS limits (Fig.18∼ Fig.20), the maximum acceptable sheet resistance is selected to be 1.4Ω/□.

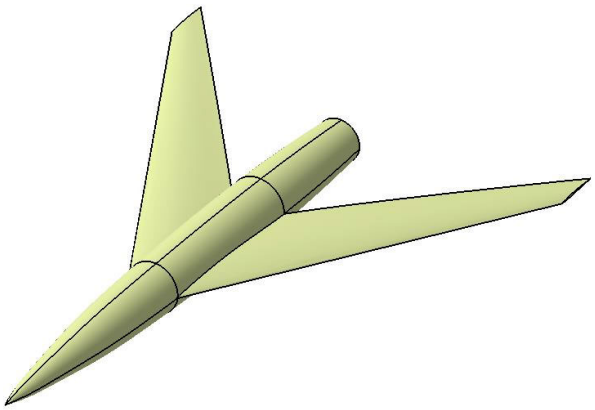

FIGURE 17. Wing-body combination model.

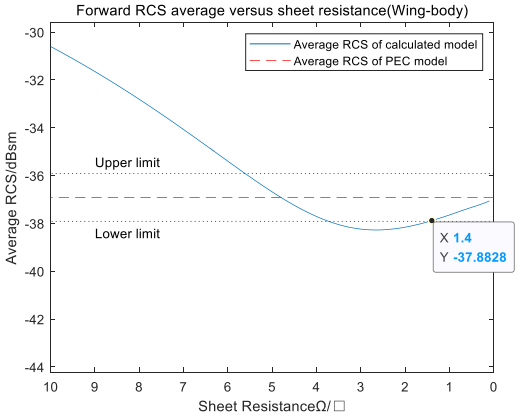

FIGURE 18. Forward RCS average versus sheet resistance (Wing-body).

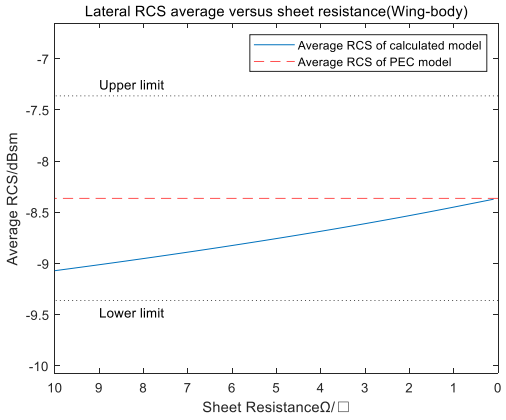

FIGURE 19. Lateral RCS average versus sheet resistance (Wing-body).

5) VARIATION OF AVERAGE RCS OF STEALTH AIRCRAFT WITH SHEET RESISTANCE

The stealth aircraft model with a length of 1.025 meters and a wingspan of 0.683 meters are shown in Fig.21. The maximum acceptable sheet resistance is selected to be 8.9Ω/□ based on the forward, lateral, and backward RCS limitations (Fig.22∼ Fig.24).

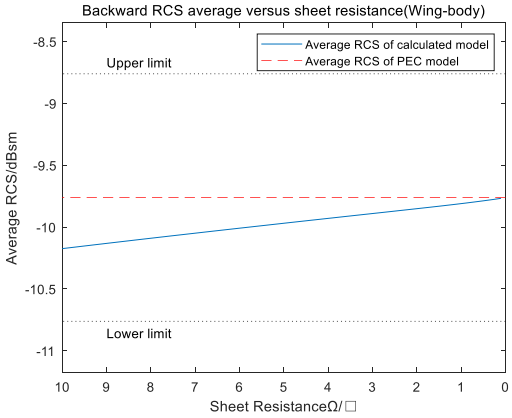

FIGURE 20. Backward RCS average versus sheet resistance (Wing-body).

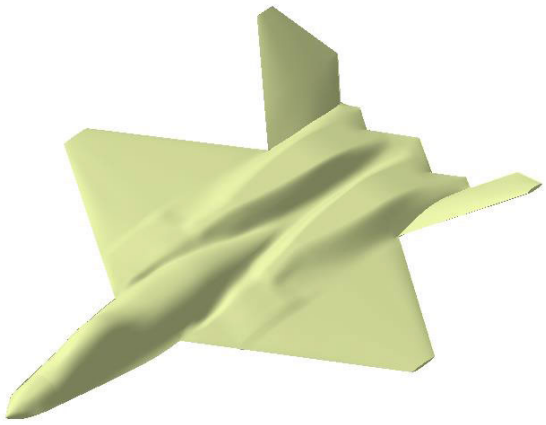

FIGURE 21. Stealth aircraft model.

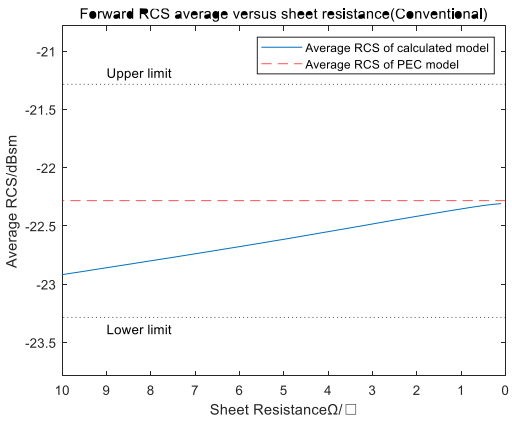

FIGURE 22. Forward RCS average versus sheet resistance (Stealth).

B. INFLUENCE OF FREQUENCY ON SURFACE CONDUCTIVITY REQUIREMENTS

In order to clarify the influence of frequency on the model's surface conductivity requirements, in this part, the shape of flying wing aircraft with stricter sheet resistance requirements is selected for analysis at multiple frequencies, as

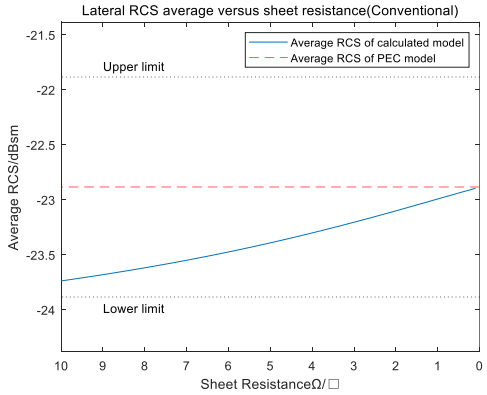

FIGURE 23. Lateral RCS average versus sheet resistance (Stealth).

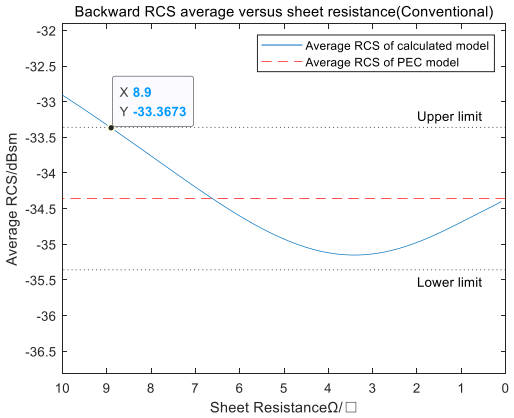

FIGURE 24. Backward RCS average versus sheet resistance (Stealth).

illustrated in Fig.25. The curves of average RCS versus sheet resistance are plotted when the electromagnetic wave frequency is in P-band, L-band, S-band, C-band and X-band [21], and the maximum acceptable sheet resistance of flying wing aircraft is summarized for each frequency band, as shown in Table 4.

TABLE 4. Maximum acceptable sheet resistance of different frequency bands.

	Average RCS	Maximum sheet resistance	Average RCS	Maximum sheet resistance
	P-band		L-band	
Forward	-14.43	9.2	-23.39	7.3
Lateral	-16.34	All	-26.55	8.4
Backward	-16.60	8.1	-25.45	6.2
	S-band		C-band	
Forward	-33.55	All	-40.23	4.2
Lateral	-33.97	All	-37.22	6.2
Backward	-35.23	9.5	-39.87	5.9
	X-band			
Forward	-44.05	3.4	Note: "All" means that the sheet	
Lateral	-38.36	4.3	resistance within the calculation	
Backward	-44.34	1.5	range is acceptable	

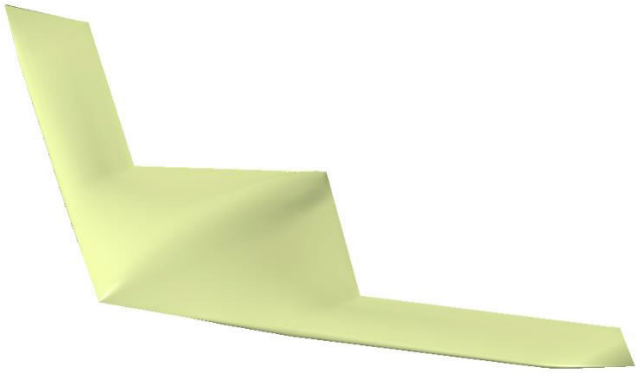

FIGURE 25. Flying wing aircraft model.

TABLE 5. Calculated frequency and wingspan of flying wing aircraft.

band	P-band	L-band	S-band	C-band	X-band
Frequency	300MHz	1GHz	3GHz	6GHz	10GHz
Wingspan	7 meters	2 meters	1.5 meters	1.5 meters	1.5 meters

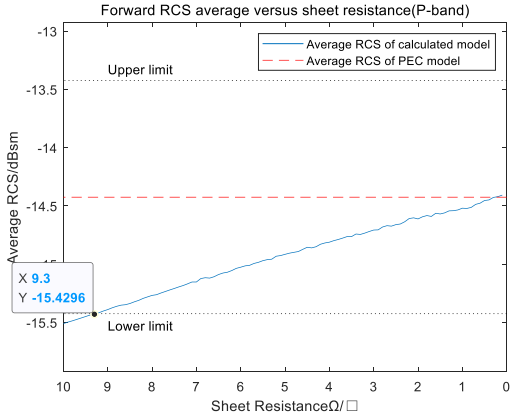

FIGURE 26. Forward RCS average versus sheet resistance (P-band).

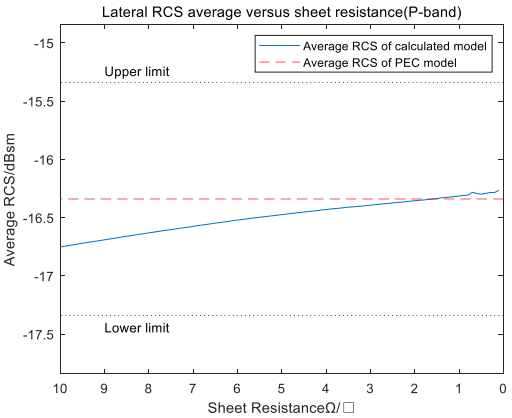

FIGURE 27. Lateral RCS average versus sheet resistance(P-band).

As frequency increases, the model's average RCS decreases, and the surface conductivity requirements also

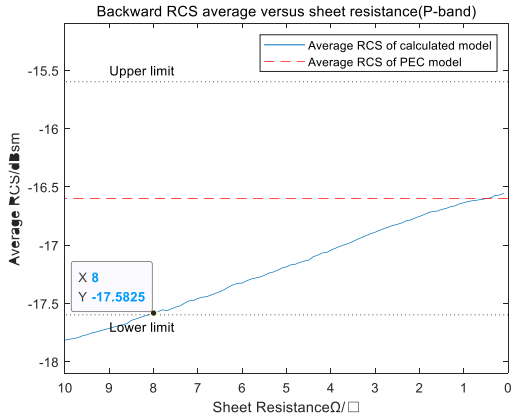

FIGURE 28. Backward RCS average versus sheet resistance(P-band).

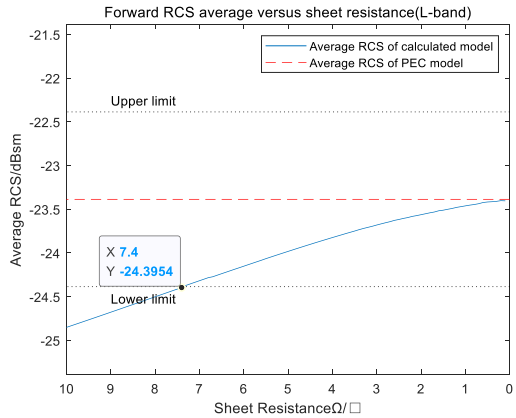

FIGURE 29. Forward RCS average versus sheet resistance (L-band).

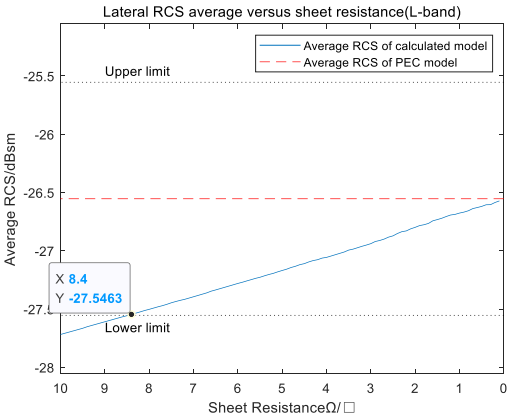

FIGURE 30. Lateral RCS average versus sheet resistance(L-band).

increase. Among all the calculation bands, X-band has the most stringent sheet resistance requirement, which is 1.5Ω/□, and the corresponding average RCS is −44.33dBsm; For the case where the average RCS is relatively high (above −30dBsm), the most stringent sheet

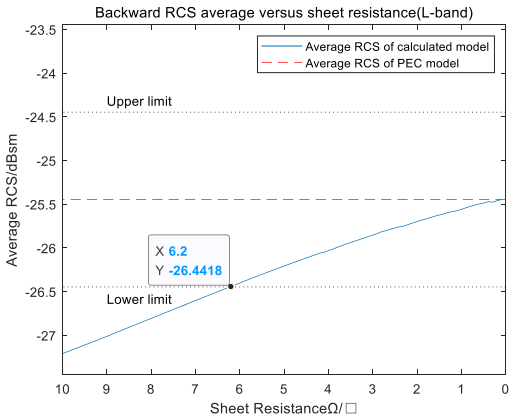

FIGURE 31. Backward RCS average versus sheet resistance(L-band).

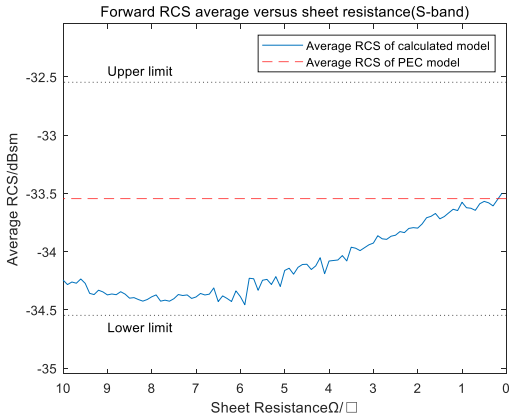

FIGURE 32. Forward RCS average versus sheet resistance (S-band).

resistance is 6.2Ω/□, and the corresponding average RCS is −25.45dBsm.

1) VARIATION OF AVERAGE RCS WITH SHEET RESISTANCE AT DIFFERENT FREQUENCIES

Considering the geometric size requirements of the high-frequency region corresponding to each band, the size of the simulation model of the flying wing aircraft will vary at different frequencies, but the shape remains unchanged, as shown in Fig.25. The calculated frequency and wingspan under each band are displayed in Table 5. The curves of the forward, lateral, and backward RCS vary with sheet resistance are respectively illustrated in Fig.26∼Fig.28 (P-band), Fig.29∼Fig.31 (L-band), Fig.32∼Fig.34 (S-band), Fig.35∼Fig.37 (C-band), Fig.38∼Fig.40 (X-band).

IV. SUGGESTIONS FOR SURFACE CONDUCTIVITY OF RCS TEST MODEL

In section 3, a simulation study is performed for several typical shapes at multiple frequencies, and the acceptable sheet resistance range for the simulation model within an error of ±1dB is clarified. RCS test models are diverse and surface resistance control standards of the model cannot be

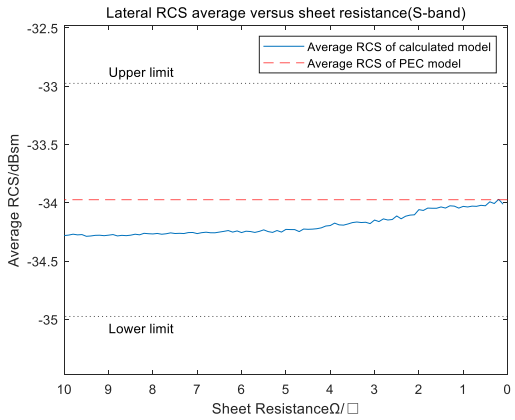

FIGURE 33. Lateral RCS average versus sheet resistance(S-band).

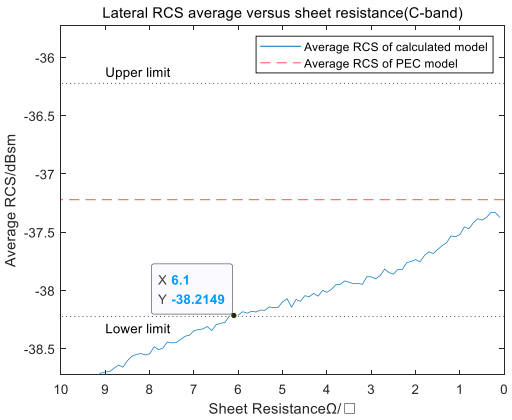

FIGURE 36. Lateral RCS average versus sheet resistance(C-band).

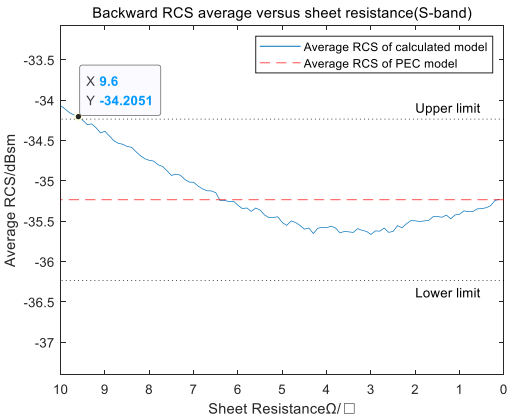

FIGURE 34. Backward RCS average versus sheet resistance(S-band).

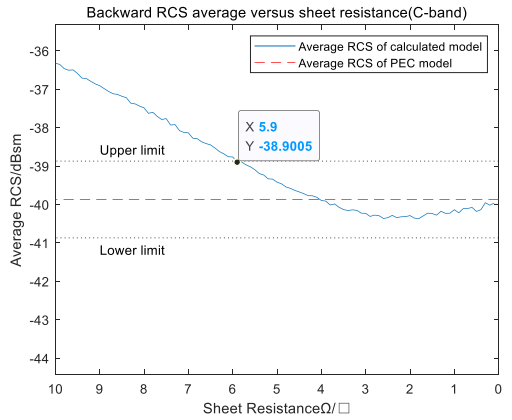

FIGURE 37. Backward RCS average versus sheet resistance(C-band).

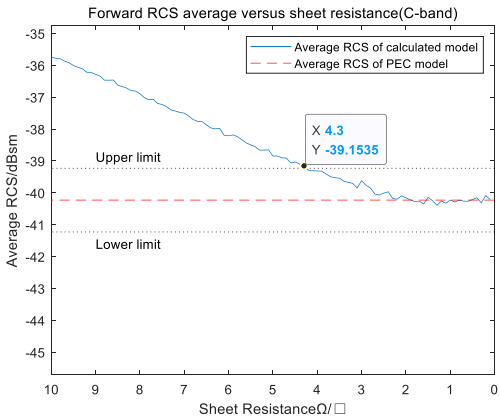

FIGURE 35. Forward RCS average versus sheet resistance (C-band).

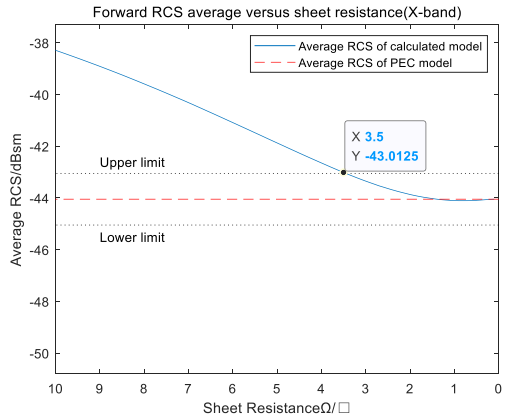

FIGURE 38. Forward RCS average versus sheet resistance (X-band).

established for a specific shape. Therefore, by comparing the simulation results of five typical shapes at various frequencies, which are summarized in Table 3 and Table 4, the case with the highest requirements for sheet resistance is selected as the surface resistance control standard of the test model. Since the higher the average RCS of the model, the lower the requirement for sheet resistance, two surface resistance control standards are developed with −30dB as the dividing line.

Utilizing the analysis results above and considering that the standard should be universal, a more accessible surface resistance control standard for the RCS test model is formulated as follows:

1. According to the conductivity requirements of the five typical shapes indicated in Table 3, the first standard is

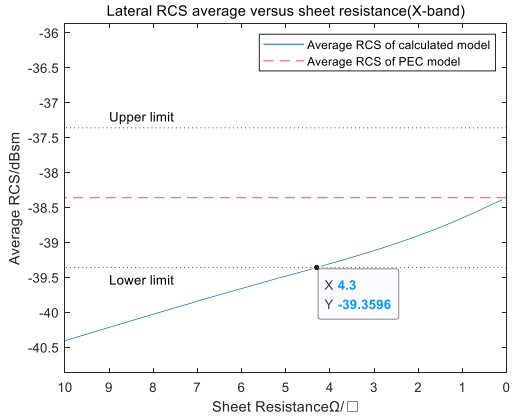

FIGURE 39. Lateral RCS average versus sheet resistance(X-band).

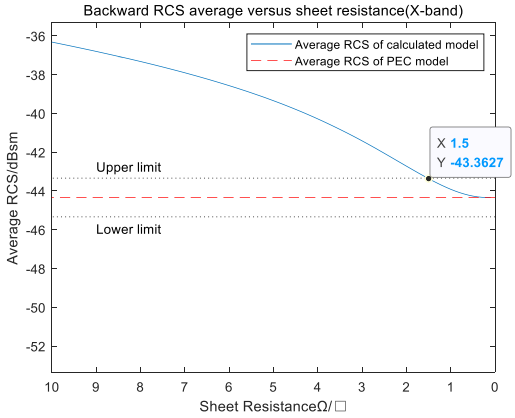

FIGURE 40. Backward RCS average versus sheet resistance(X-band).

conservatively proposed as: **The sheet resistance of the model surface should not exceed 1.4Ω/□ when the average RCS of the model is lower than −30dBsm**, which is 93% relaxed compared to the Chinese military standard.

2. According to the conductivity requirements of the five frequencies indicated in Table 4, the second standard is conservatively proposed as: **The sheet resistance of the model surface should not exceed 6Ω/□ when the average RCS of the model is higher than −30dBsm**, which is 727% relaxed compared to the Chinese military standard.

V. CONCLUSION

In order to elucidate the influence of the surface conductivity of the model on the radar scattering characteristics, the RCS analysis method for the finite conductivity model is established by theoretical, simulation and experimental research. The simulation analysis of radar scattering characteristics under different sheet resistances and multiple frequencies is carried out using a variety of typical shapes such as the sphere, cube, flying wing aircraft, wing-body configuration, and stealth aircraft as research objects.

The conclusions are as follows:

(1) The influence of sheet resistance of the model surface on the radar scattering characteristics is analyzed quantitatively.

(2) The RCS simulation method of the finite conductivity model is established based on computational electromagnetics.

(3) The RCS test is performed on ITO conductive films with different sheet resistances in a compact range. The simulation value of RCS is basically the same as the test value.

(4) The surface conductivity control standard of the RCS test model, which takes into account the conductivity requirements of various shapes and multiple frequencies, can be summarized as follows: **The sheet resistance of the model surface should not exceed 1.4Ω/□ or 6Ω/□ for models with average RCS less than or higher than −30dBsm**, which is 93% and 727% relaxed compared to that of the Chinese military standard.

REFERENCES

[1] A. Ramya and V. S. Leela, "3D printing technologies in various applications," *Int. J. Mech. Eng. Technol.*, vol. 7, no. 3, pp. 396–409, 2016.
[2] C.-C. Kuo and M.-R. Li, "A cost-effective method for rapid manufacturing sheet metal forming dies," *Int. J. Adv. Manuf. Technol.*, vol. 85, nos. 9–12, pp. 2651–2656, Aug. 2016.
[3] *GJB5022–2001 Method for Measurement of Radar Cross Section of Scale Target Indoor Range*, AVIC China Aero-Polytechnol. Establishment, Beijing, China, 2001.
[4] N. Shahrubudin, T. C. Lee, and R. Ramlan, "An overview on 3D printing technology: Technological, materials, and applications," *Procedia Manuf.*, vol. 35, pp. 1286–1296, Jan. 2019.
[5] J. T. Kelley, A. Maicke, D. A. Chamulak, C. C. Courtney, and A. E. Yilmaz, "Adding a reproducible airplane model to the Austin RCS benchmark suite," in *Proc. Int. Appl. Comput. Electromagn. Soc. Symp. (ACES)*, Jul. 2020, pp. 1–2.
[6] T. C. Zhang, Y. F. Wang, L. J. Feng, and K. Zhang, "Applied research of conductive coating in composite radar target characteristics control," *Packag. Eng.*, vol. 33, no. 3, pp. 142–145, 2012.
[7] M. Ezuma, M. Funderburk, and I. Guvenc, "Compact-range RCS measurements and modeling of small drones at 15 GHz and 25 GHz," in *Proc. IEEE Radio Wireless Symp. (RWS)*, Jan. 2020, pp. 313–316.
[8] S. H. Liu, J. M. Liu, X. L. Dong, and Y. P. Duan, *Electromagnetic Wave Shielding and Absorbing Materials*. Beijing, China: Chemical Industry Press, 2013.
[9] E. F. Knott, J. F. Schaeffer, and M. T. Tulley, *Radar Cross Section*. Raleigh, NC, USA: SciTech, 2004.
[10] L. Y. Khaliulin and S. A. Tretýakov, *Radiotekh*, vol. 43. Moscow, Russia: Élektron, p. 16, 1998.
[11] I. V. Antonets, L. N. Kotov, S. V. Nekipelov, and E. N. Karpushov, "Conducting and reflecting properties of thin metal films," *Tech. Phys.*, vol. 49, no. 11, pp. 1496–1500, 2004.
[12] S. Swann, "Magnetron sputtering," *Phys. Technol.*, vol. 19, no. 2, p. 67, 1988.
[13] N. V. Venkatarayalu, W. W. Lee, D. Tan, and C. B. Soh, "Effect of resistivity of ITO thin film when used in transparent checkerboard surfaces for RCS reduction," in *Proc. Prog. Electromagn. Res. Symp.-Fall (PIERS-FALL)*, 2017, pp. 473–476.
[14] X. Kong, S. Jiang, L. Kong, Q. Wang, H. Hu, X. Zhang, and X. Zhao, "Transparent metamaterial absorber with broadband RCS reduction for solar arrays," 2020, *arXiv:2003.13005*.
[15] J. Z. Ji, P. L. Huang, Y. P. Ma, and S. J. Zhang, *The Principle of Stealth*. Beijing, China: Beihang Univ. Press, 2018.
[16] P. Eskelinen and P. Harju, "Low cost arrangements for scale model RCS and pattern measurements," in *Proc. NAECON*, vol. 2, Jul. 1997, pp. 827–830.
[17] L. Sevgi, Z. Rafiq, and I. Majid, "Radar cross section (RCS) measurements," *IEEE Antennas Propag. Mag.*, vol. 55, no. 6, pp. 277–291, Dec. 2013.
[18] Y. C. Wu, J. Huang, and L. Song, "Research on the relationship between resistivity and resistance between two points on RCS test model," to be published.

[19] S. B. Kondawar and P. R. Modak, "Theory of EMI shielding," in *Materials for Potential EMI Shielding Applications*. Amsterdam, The Netherlands: Elsevier, Jan. 2020, pp. 9–25.
[20] T. Watanabe and Y. Akamine. (2022). *Low-Cost Radar Cross-Section Measurement With a Resin-Made Model Coated With Conductive Paste*. TechRxiv. [Online]. Available: https://doi.org/10.36227/techrxiv.Z21127765.v1
[21] M. Skolnik, "An introduction and overview of radar," *Radar Handbook*. New York, NY, USA: McGraw-Hill, Feb. 2008.

WU YACONG was born in Hebei, China, in 1992. She received the B.S. degree in aircraft design and engineering from Xi'an Jiaotong University, Xi'an, China, in 2015, and the M.S. degree in aircraft design from Beihang University, Beijing, China, in 2018, where she is currently pursuing the Ph.D. degree in aircraft design with the Department of Aeronautical Science and Engineering.

Her research interests include radar stealth technology of aircraft, parameterization and aerodynamic optimization of aircraft, and scaled flight test simulation of aircraft.

HUANG JUN received the B.S. degree in aircraft design from Shenyang Aerospace University, Shenyang, China, in 1986, and the M.S. and Ph.D. degrees in aircraft design from Beihang University, Beijing, China, in 1997 and 2000, respectively.

He is currently a Professor at Beihang University. His research interests include aircraft conceptual design, aircraft low-observability design, and aircraft operation effectiveness analysis.

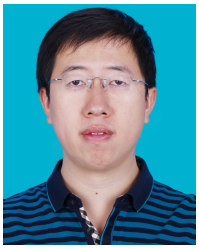

SONG LEI received the B.S. degree in aircraft design and engineering and the M.S. and Ph.D. degrees in aircraft design from Beihang University, Beijing, China, in 2009, 2010, and 2015, respectively.

He is currently an Associate Professor at Beihang University. His research interests include aircraft conceptual design and optimization and radar stealth technology of aircraft.

Prof. Song is a Youth Editorial Board Member of *Aerospace Knowledge* and *Model Airplane News*.